Desalination and Water Treatment
www.deswater.com
doi: 10.1080/19443994.2015.1049961

57 (2016) 12192–12203
June

Taylor & Francis
Taylor & Francis Group

Design and model parameters estimation for fixed–bed column adsorption of Cu(II) and Ni(II) ions using magnetized saw dust

Meghna Kapur, Monoj Kumar Mondal*

Department of Chemical Engineering and Technology, Indian Institute of Technology (Banaras Hindu University), Varanasi 221005, Uttar Pradesh, India, email: meghnakapur07@gmail.com (M. Kapur), Tel. +91 9452196638; Fax: +91 5422367098; email: mkmondal13@yahoo.com (M.K. Mondal)

Received 10 November 2014; Accepted 3 May 2015

ABSTRACT

Fixed-bed column studies were performed using magnetized sawdust (Fe_3O_4–SD) as adsorbent for removal of Cu(II) and Ni(II) ions form aqueous solutions. Breakthrough curves were obtained by performing experiments in order to evaluate the influence of adsorbent bed height (2, 4, 8 cm), metal ion concentration in feed solution (10, 20, 30 mg/L), and feed flow rate (15, 20, 25 mL/min) for adsorption of Cu(II) and Ni(II) ions onto Fe_3O_4–SD adsorbent. Adsorption kinetics was analyzed using Bohart–Adams, Thomas, and Yoon–Nelson models. Kinetic data correlated well with both Thomas and Yoon–Nelson models, while Bohart–Adams model poorly predicted the model operation. Saturation loading capacity of adsorbent bed decreased with increase in adsorbent bed height, metal concentration in feed, and feed flow rate. Both mass transfer zone (MTZ) height and height of unused bed (H_{UNB}) noticeably increased with increase in the values of the parameter studied. The results showed that reduced MTZ height and lowest H_{UNB} are suitable for operating the column satisfactorily.

Keywords: Fixed-bed adsorption; Cu(II) and Ni(II); Fe_3O_4–SD; Saturation loading capacity; H_{UNB} and MTZ

1. Introduction

The existence of heavy metal ions in industrial discharges causes serious environmental threat as they are persistent and cannot be degraded [1,2]. Metals categorized as heavy metals (density ≥ 6 g/cm^3) act as micronutrients for both humans and plants up to a certain level but their accumulation results into carcinogenic effects. Both Cu(II) and Ni(II) are present in effluents of large number of industries. Copper along with arsenic and mercury is considered as the highest toxic species to the mammalians [3]. In humans, copper is required for proper functioning of certain enzymes, viz. ceruloplasmin, tyrosinase [4]. It is also associated with melanin formation and iron metabolism but a higher dose causes liver and kidney damage, gastrointestinal catarrh, and even leads to genetic abnormalities. Similarly, nickel-induced toxicity includes dermatitis, lung fibrosis, cardiovascular, kidney diseases, and even cancer. It inhibits the activity of oxidative enzymes. The toxicity of nickel to both humans as well as the environment is very well known. Once nickel enters the body, its chemical form may change but it cannot be destroyed. High

*Corresponding author.

concentration of Ni(II) causes cancers of lungs, nose, and bone. For plants, the margin between deficiency and toxicity is quite narrow [5]. Copper is required for chlorophyll production, respiration, and protein synthesis but when present in excess, signs of chlorosis, stunted growth, and delayed maturity are noticed. While proper seed germination and metabolism [6] are dependent on Ni, excess of which can cause chlorosis and displacement of Fe from important centers. Thus, their elimination from industrial wastewaters is becoming an important challenge for industry in relation with increasingly drastic national and international regulations [7]. Discharge of various industries like electroplating industries has high amount of Cu(II) and Ni(II) ions [8], which should be removed to meet the discharge standards. The conventional methods mostly have a limit of minimum 100 mg/L of metal concentration, but adsorption can remove even the traces. Fixed-bed column is widely used in the industry for adsorption operation. Actual applications of adsorption imply the use of continuous flow processes. The packed bed or fixed-bed adsorption columns are the most suitable systems for the removal of heavy metals as they are simple to operate, attain a high yield, and can be easily scaled up for testing at pilot- or industrial-scale. In comparison with batch studies, there have been few dynamic biosorption studies [9]. Although a number of investigations have been carried out in fixed-bed arrangement on the adsorption of Cu(II) ions onto coconut-shell [10], chitosan immobilized on bentonite [11], zeolite/cellulose acetate blend fiber [12], rice husk-based activated carbon [13] to name a few. Similarly, Ni(II) ions sorption was studied onto activated carbon obtained from sugarcane bagasse pith [14] and tea factory waste [15]. Agricultural waste chosen for the present work was *Mangifera indica* sawdust. It has the potential of adsorbing heavy metal ions from aqueous solutions even in the form available. But properties of adsorbent need to be improved for treating the solution of more than one heavy metal efficiently by enhancing surface area of active sites of this adsorbent, and the magnetic behavior of particle formed is quite useful in phase (solid–liquid) separation. The adsorbent of this study was prepared by impregnating magnetic properties into sawdust by coprecipitating it with $FeCl_3{\cdot}6H_2O$ and $FeSO_4{\cdot}7H_2O$. Due to the crystallinity developed in the particles, the size could be reduced thereby enhancing the surface area and in turn the availability of adsorptive sites increased. The studies performed by many researchers were mainly focused on some chemical treatments of adsorbents. Modifications through citric acid, phosphoric acid [16], and sodium sulfide [17] have been proved suitable for adsorbing cations earlier but no such treatment suited adsorption of two heavy metals simultaneously from the solution. The novelty of this work lies in combined removal of Cu(II) and Ni(II) ions from the aqueous solutions using Fe_3O_4–SD as adsorbent in a fixed-bed column which has not been attempted earlier. The experimental results have been analyzed through saturation loading, height of unused bed (H_{UNB}), and mass transfer zone (MTZ) studies for its applicability to industrial-scale operation.

2. Material and methods

2.1. Preparation of Fe_3O_4–SD adsorbent

Sawdust collected from a sawmill was washed several times with double distilled water, dried, and then sieved to obtain particles with average particle size of 96.5 μm [18]. The Fe_3O_4–SD adsorbent was prepared by coprecipitating 1 g of sawdust with 6.1 g $FeCl_3{\cdot}6H_2O$ and 4.2 g $FeSO_4{\cdot}7H_2O$ along with the addition of 10 ml of ammonium hydroxide [19]. Precipitate formation occurred at pH 10 and temperature of 80°C. Black precipitate obtained was filtered, dried, and crushed to nano-range particles.

2.2. Reagents

All the prime chemicals used for experimentation were of analytical grades. A stock solution of 1,000 mg/L of Cu(II) and Ni(II) was prepared by dissolving 3.802 g cupric nitrate [$Cu(NO_3)_2{\cdot}3H_2O$] and 6.73 g ammonium nickel(II) sulfate [$(NH_4)_2SO_4{\cdot}NiSO_4{\cdot}6H_2O$] in 1.0-L double distilled water. Successive dilutions of the stock solutions were done to obtain the required concentrations of Cu(II) and Ni(II), respectively, in aqueous samples.

2.3. Experimental setup

A glass column of length 30 and 2.54 cm internal diameter, filled with weighed amount of adsorbent was used as a fixed-bed adsorber. The column was packed with adsorbent between two layers of glass wool and a glass bead layer (Fig. 1). Glass wool provided at the bottom also acts as a filter aid. The adsorbent was added from the top of the column and allowed to settle by gravity force. The upper portion of the adsorbent was covered with glass beads to ensure proper distribution of the inlet stream. Synthetic wastewater was fed into the column through a peristaltic pump at a controlled flow rate. The studies of adsorption with two adsorbates Cu(II) and Ni(II) on Fe_3O_4–SD were carried out in the feed flow rate range

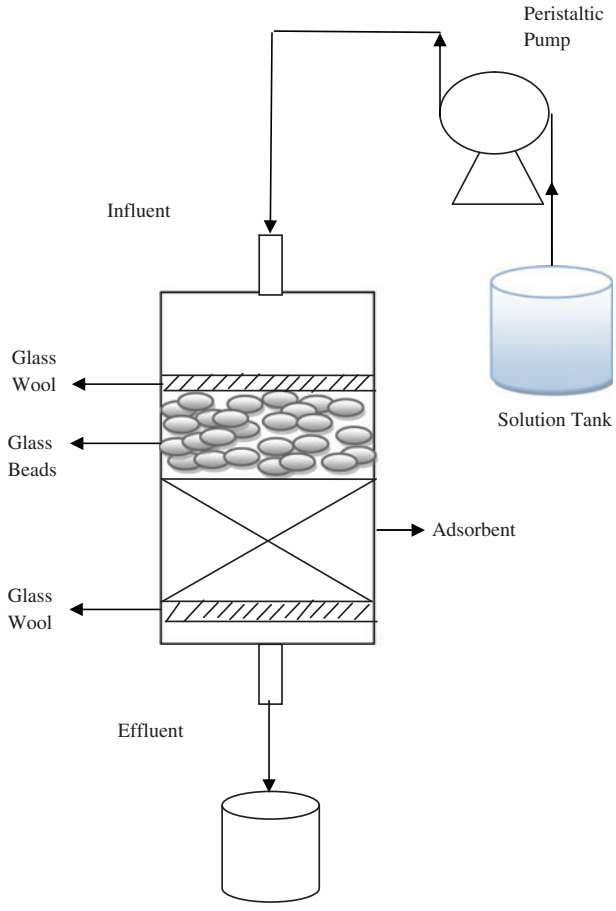

Fig. 1. The schematic of the fixed-bed adsorption column for experimental study.

(15–25 mL/min), metal concentrations in feed (10–30 mg/L), and adsorbent bed height (2–8 cm) at room temperature and pH 5. Samples were collected at regular intervals and analyzed for the residual metal (Cu(II) and Ni(II)) concentration by following standard methods [20] using UV–visible spectrophotometer (ELICO SL 159 UV–vis Spectrum). The sodium dimethyldithiocarbamate with ammoniacal solution in the presence of Cu(II) ions in aqueous solution produces yellowish color. Absorbance of these solutions was read at wavelength of 457 nm. Dimethylglyoxime (DMG) forms a red colored complex when treated with an alkaline solution of nickel in the presence of an oxidizing agent such as bromine. The absorbance of colored complex was read at wavelength of 445 nm.

3. Analysis of fixed-bed adsorption column data

The appearance time for breakthrough and its shape are important characteristics for determining the dynamic response of fixed-bed adsorption column. The breakthrough time (t_b) is defined as the time at which metal concentration in the effluent (C_t) reaches 1% of the inlet concentration (C_o), and bed exhaustion time (t_e) is the time at which metal concentration in the effluent exceeds 99% of C_o. The breakthrough curve is represented as the ratio of effluent metal concentration to inlet metal concentration (C_t/C_o) as a function of time or volume of effluent for a given bed height [21]. Effluent volume (V_{eff}) can be calculated from Eq. (1):

$$V_{eff} = Qt_{total} \tag{1}$$

where t_{total} and Q are the total flow time (min) and volumetric flow rate (mL/min). The total adsorbed metal quantity q_{total} (mg) in the column for a given feed concentration and flow rate (Q) is calculated from Eq. (2):

$$q_{total} = \frac{Q}{1,000}\int_0^{t_{total}} C_{ad}\,dt = \frac{QA}{1,000} \tag{2}$$

where $C_{ad} = (C_o - C_t)$ is the adsorbed metal concentration (mg/L) at time t. The computer program ORIGIN 8.1 was used to calculate (by numerical integration) the area under the curve.

Saturation loading capacity of the adsorbent bed or equilibrium metal uptake q_e (mg/g) in the column is calculated as the following:

$$q_e = \frac{q_{total}}{m} \tag{3}$$

where m is the dry mass of adsorbent in the column (g).

Time equivalent to the total or stoichiometric capacity of the bed t_t is obtained by following numerical integration as given below:

$$t_t = \int_0^{\infty}\left(1 - \frac{C}{C_o}\right)dt \tag{4}$$

Time equivalent to the usable capacity of the bed t_u is given as:

$$t_u = \int_0^{t_b}\left(1 - \frac{C}{C_o}\right)dt \tag{5}$$

The H_{UNB} can be found as:

$$H_{UNB} = \left(1 - \frac{t_u}{t_t}\right) H_T \quad (6)$$

where H_T is total bed height of the adsorbent for the column.

MTZ is the region or zone where metal is actually being adsorbed onto active surface of the adsorbent. The MTZ moves from the inlet toward the outlet of the fixed-bed during operation as adsorption proceeds. The MTZ height is represented as:

$$\text{MTZ} = \frac{H_T}{\left(\frac{t_t}{t_t - t_b}\right) - \beta} \quad (7)$$

where $\beta = \frac{t_u}{t_t}$ represents the degree of saturation in the MTZ.

Velocity of stoichiometric front u_t can be calculated as:

$$u_t = \frac{H_T}{t_t} \quad (8)$$

4. Results and discussion

4.1. Characterization of Fe_3O_4–SD adsorbent

The transmission electron microscopy analysis revealed smaller and compact particles of Fe_3O_4–SD with average particle diameter 50 nm. The BET surface area obtained was 41.7414 m^2/g. The X-ray diffraction (XRD) demonstrated high crystallinity of Fe_3O_4–SD nano-particles. Phase of Fe_3O_4 was revealed from the patterns of the XRD obtained (figure not shown). Major peaks of pure Fe_3O_4 with inverse spinel structure were visualized at 30.1°, 35.5°, 43.1°, 53.4°, 57.0°, and 62.6° with their respective indices (2 2 0), (3 1 1), (4 0 0), (4 2 2), (5 1 1), and (4 4 0) in consistency with the database in JCPDS file (PCPDFWIN v.2.02, PDF No. 85-1436). It was analyzed from the Fourier transform infrared spectroscopy spectra (before adsorption) of Fe_3O_4–SD nanoparticles that it exhibits strong bands of iron oxide in the low frequency region (1,000–400 cm^{-1}) due to the iron oxide skeleton. This supports complete association of sawdust with magnetic Fe_3O_4 particles. Spectroscopic bands shift (after adsorption) indicated the possible involvement of

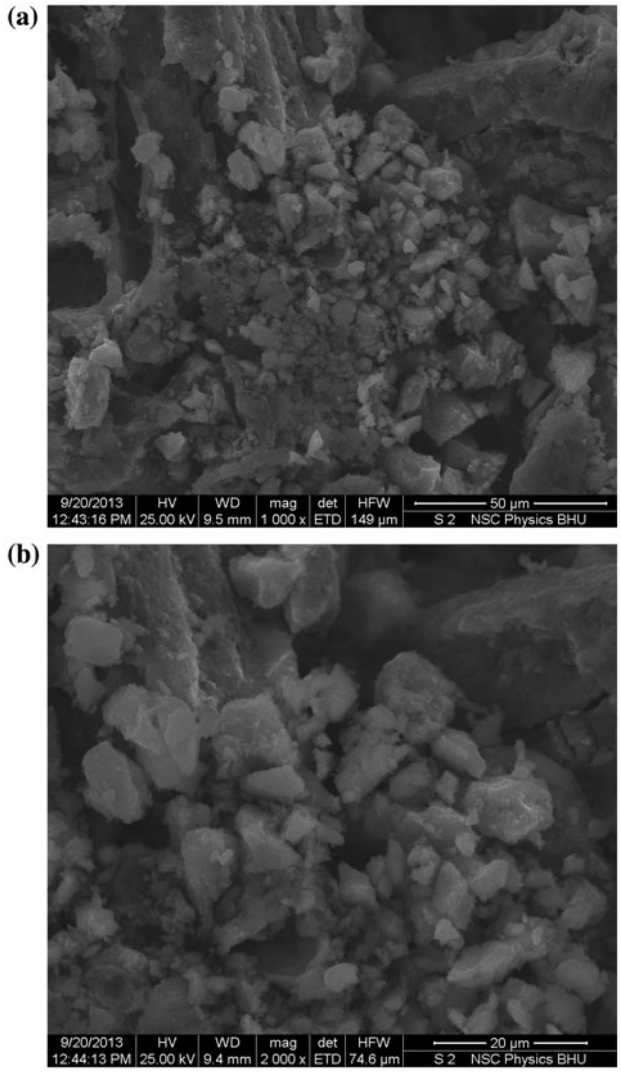

Fig. 2. SEM micrographs of Fe_3O_4–SD at different magnifications (a) 1,000× and (b) 2,000×.

Table 1
Spectral analysis of Fe_3O_4–SD nanoparticles before and after adsorption of Cu(II) and Ni(II) ions

Band positions (cm^{-1})			
Before adsorption	After adsorption	Differences	Assignment
584.1	581.7	+2.4	Fe–O bonds
428.9	407	+21.9	–Fe–O bonds
3,453.1	3,180.5	+272.6	–OH stretching vibrations

Fe–O and –OH bonds in the adsorption activity (Table 1). Through the scanning electron microscopy (SEM) micrographs of Fe_3O_4–SD at different magnifications (Fig. 2), it is evident that sawdust surface is completely covered with iron oxide to form irregular structure with sufficient pores for carrying out the adsorption mechanism. All iron oxide particles are closely bound to form irregular cage-like structure.

4.2. Influence of operating parameters on adsorption

In order to validate the combined adsorption of Cu (II) and Ni(II) ions from aqueous solutions using Fe_3O_4–SD as adsorbent, a fixed-bed column was used to carry out the experimental runs. Variations of parameters were investigated as adsorbent bed height, feed flow rate, and metal ion concentration in feed solution to evaluate adsorption capacity, H_{UNB} and MTZ of the column.

4.2.1. Effect of adsorbent bed height

Metal uptake by adsorbent in fixed-bed column mainly depends upon the height of adsorbent bed in the column. The Fe_3O_4–SD particles were fed into the column to accomplish a bed height of 2, 4, and 8 cm.

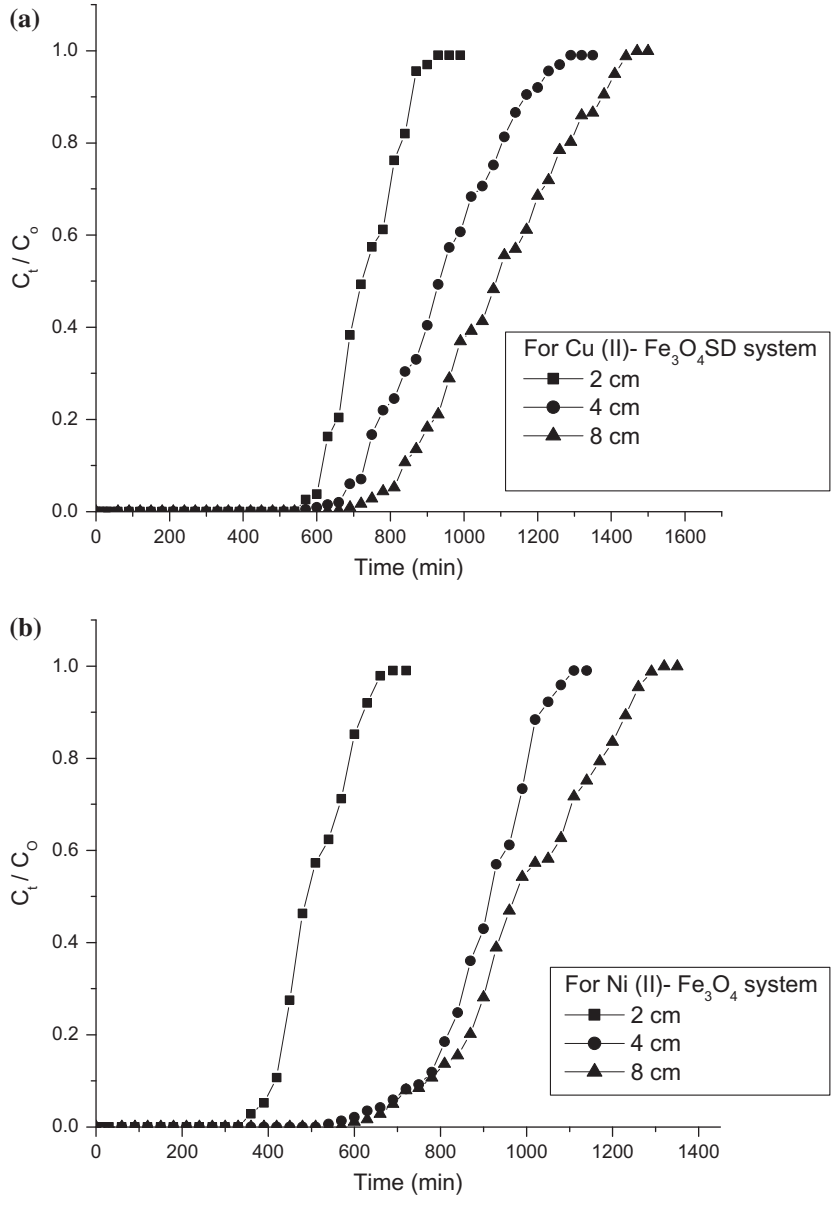

Fig. 3. Breakthrough curves at different adsorbent bed heights for (a) Cu(II) and (b) Ni(II) adsorption onto Fe_3O_4–SD.

Table 2
Experimental data analysis for adsorption of (a) Cu(II) and (b) Ni(II) onto Fe_3O_4–SD in a fixed-bed column at different process conditions

C_o (mg/L)	Q (mL/min)	Z (cm)	t_b (min)	t_{total} (min)	q_{total} (mg)	q_e ± S.D. (mg/g)	V_{eff} (ml)	MTZ (cm)	H_{UNB} (cm)	u_t (cm/min)
(a)										
10	20	2	551.2	735.7	147.1	29.42 ± 1.9	14,714.0	0.61	0.50	0.0027
10	20	4	604.7	943. 0	188.5	18.85 ± 1.3	18,859.2	1.86	1.43	0.0042
10	20	8	692.8	1,094.2	218.8	10.94 ± 1.9	21,884.0	3.82	2.93	0.0073
10	15	2	751.4	1,063.2	159.4	31.89 ± 2.1	15,948.0	0.74	0.58	0.0018
10	20	2	551.2	735.7	147.1	29.42 ± 1.9	14,714.0	0.61	0.50	0.0027
10	25	2	247.9	530.7	132.6	26.53 ± 1.2	13,267.5	1.41	1.06	0.0037
10	15	2	751.4	1,063.2	159.4	31.89 ± 2.1	15,948.0	0.74	0.58	0.0018
20	15	2	250.2	455.3	136.6	27.31 ± 1.8	6,828.8	1.19	0.90	0.0043
30	15	2	105.6	276.7	124.4	24.89 ± 2.2	4,149.7	1.61	1.23	0.0072
(b)										
10	20	2	340.7	507.9	101.5	20.31 ± 1.5	10,157.6	0.84	0.66	0.0034
10	20	4	558.4	904.3	180.8	18.08 ± 1.2	18,085.0	2.00	1.53	0.0044
10	20	8	596.5	997.1	199.4	9.97 ± 2.1	19,942.6	4.23	3.21	0.0080
10	15	2	480.6	786.4	117.9	23.59 ± 1.3	11,796.5	1.02	0.78	0.0025
10	20	2	340.7	507.9	101.5	20.31 ± 1.5	10,157.6	0.84	0.66	0.0034
10	25	2	160.4	377.3	94.3	18.86 ± 2.2	9,431.8	1.52	0.57	0.0053
10	15	2	480.6	786.4	117.9	23.59 ± 1.3	11,796.5	1.02	0.78	0.0025
20	15	2	161.6	336.8	101.0	20.20 ± 1.9	5,051.5	1.38	1.04	0.0060
30	15	2	51.17	210.6	94.8	18.95 ± 2.3	3,159.5	1.85	1.51	0.0090

As the particle size is in nano-range, small amount of adsorbent [22] was taken so as to avoid the condition of flooding. The breakthrough curves for both Cu(II) and Ni(II) ions at different bed heights representing adsorbent mass loadings are shown in Fig. 3. Exhaustion time and effluent volume were seen increasing with increase in adsorbent bed height, which may be due to the availability of more time for contact between adsorbate and adsorbent. For all the cases, slope of breakthrough curve decreased with increasing amount of adsorbent and resulted in broadened MTZ. Total adsorption uptakes for both the metals increased on increasing the adsorbent bed height as the presence of active sites for binding the metals increased. The trend shown by saturation loading capacities at different adsorbent bed height (2, 4, 8 cm) is as follows: 29.42, 18.85, 10.94 mg/g for Cu(II) and 20.31, 18.08, 9.97 mg/g for Ni(II) ions. The H_{UNB} increased with bed height; thus, the greater saturation loading capacity and lowest H_{UNB} for the adsorbent bed height 2 cm was found to be suitable for further studies. It was predicted from the MTZ calculations (Table 2) that the shortened MTZ height [23] corresponding to the lowest amount of adsorbent is suitable for the process.

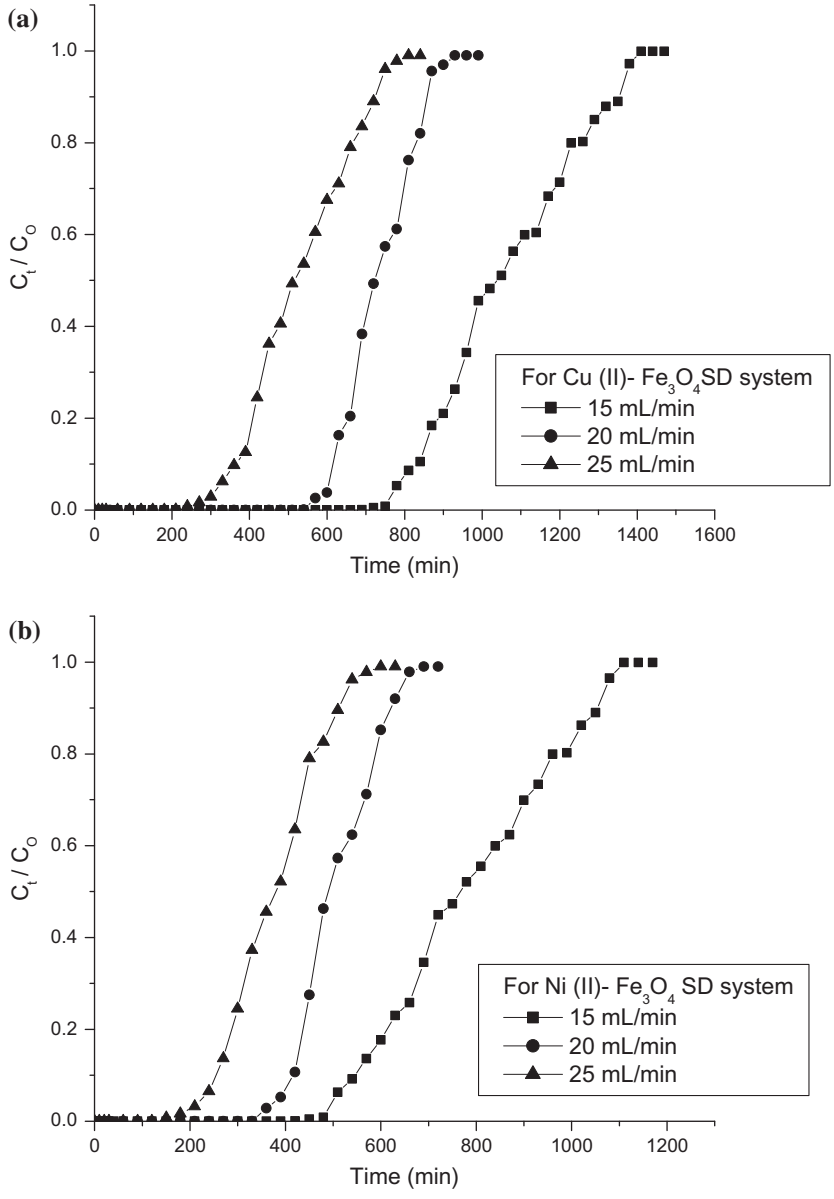

Fig. 4. Breakthrough curves at different flow rates for (a) Cu(II) and (b) Ni(II) adsorption onto Fe_3O_4–SD.

4.2.2. Effect of feed flow rate

Breakthrough curves obtained at different feed flow rates of liquid containing metal ions are shown in Fig. 4. Breakthrough occurred faster for increasing flow rates as for high feed flow rate, the adsorbate phase did not have enough time to be in contact with adsorbent particles and resulted in lower removal of Cu(II) and Ni(II) ions. The saturation loading capacities were found to be 31.89, 29.42, 26.53 mg/g for Cu (II) and 23.59, 20.31, 18.86 mg/g for Ni(II) at 15, 20, 25 mL/min feed flow rate, respectively (Table 2). At higher flow rates, the external mass transfer resistance from bulk of the liquid to the surface of adsorbent decreases, and thus, the residence time decreases resulting in lower removal. Also, the H_{UNB} and MTZ increased with increasing flow rate, implying that the column performed well for lower flow rates.

4.2.3. Effect of metal ion concentration in feed solution

Effect of Cu(II) and Ni(II) concentration in feed solution (10, 20, 30 mg/L) on performance of breakthrough curves at constant adsorbent bed height 2 cm and flow rate (15 mL/min) is depicted in Fig. 5. For

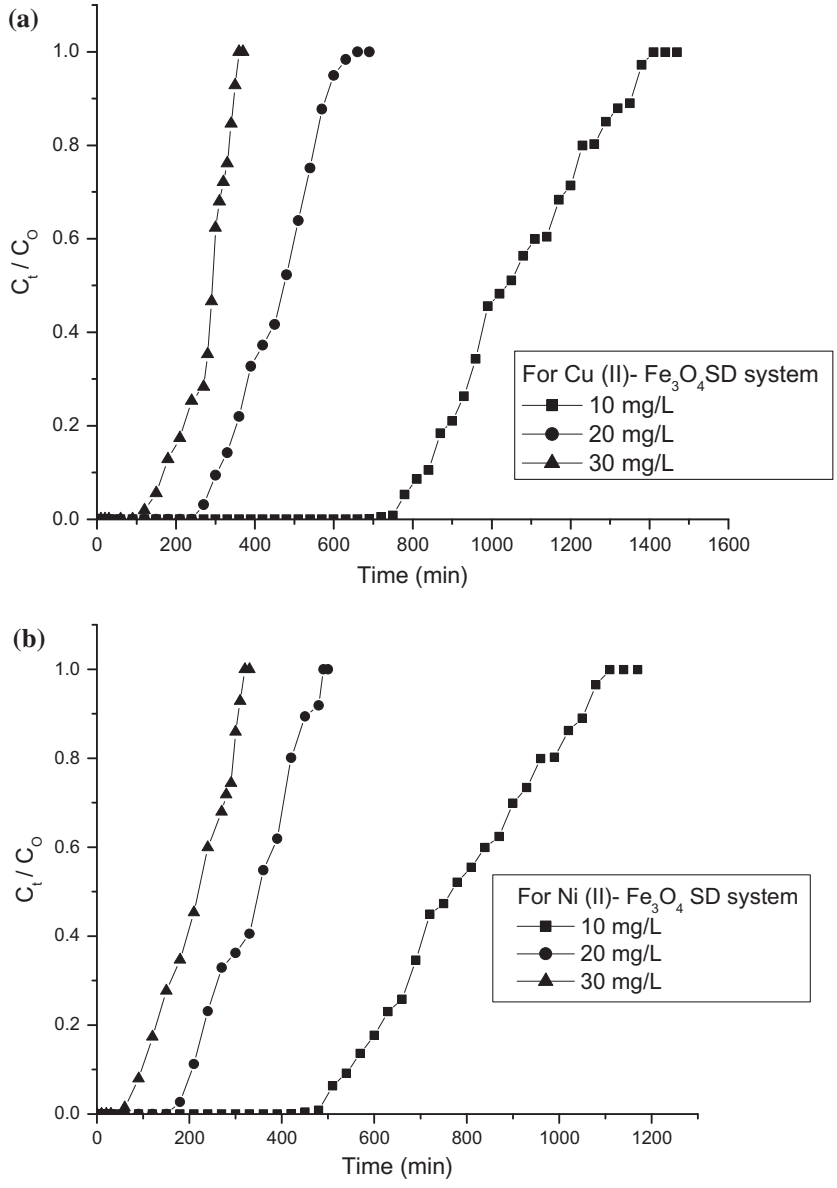

Fig. 5. Breakthrough curves at different metal ion concentrations in feed solution for (a) Cu(II) and (b) Ni(II) adsorption onto Fe_3O_4–SD.

low metal concentration in feed solution, breakthrough occurred late as lower concentration gradient caused slow transport due to decreased diffusion coefficient [24]. While at the higher metal concentration, the adsorbent got saturated earlier. The saturation loading capacity decreased from 31.89 to 24.89 mg/g for Cu(II) and 23.59 to 18.95 mg/g for Ni (II) on increasing metal concentration in feed from 10 to 30 mg/L. Therefore, the column showed good performance at lower metal concentration in feed solution which could be confirmed from increased values of H_{UNB} and MTZ with increasing concentration of metal ions in feed solution.

4.3. Dynamic modeling of experimental data

The experimental data were used to find out dynamic model parameters for adsorption of Cu(II) and Ni(II) onto Fe_3O_4–SD using well-known Bohart–Adams, Thomas, and Yoon–Nelson models particularly implied in fixed-bed column.

4.3.1. Bohart–Adams model

This model was used for the initial part of the breakthrough curve. It assumes that the adsorption equilibrium is not instantaneous and the rate of adsorption is proportional to both the residual capacity of adsorbent and the concentration of metal species [25]. This model for early stage of the breakthrough curve is given as follows:

$$\ln\left(\frac{C_t}{C_o}\right) = k_{AB}C_o t - k_{AB}C_S\left(\frac{z}{U_o}\right) \quad (9)$$

where C_o and C_t are the inlet and outlet metal concentrations, respectively, z (cm) is the bed height, U_o (cm/min) is the superficial velocity, C_S (mg/L) is the saturation concentration, and k_{AB} (L/mg min) is the Bohart–Adams model constant representing solute uptake rate. Interpretation was done through the linear regression analysis of the plots of $\ln(C_o/C_t)$ against t. The decline in the rate of uptake (k_{AB}) of both the metals with increasing adsorbent bed height and metal ion concentration in feed (Table 3) suggests that in the initial part of the adsorption, kinetics is governed by external mass transfer. Same trend was observed in earlier research [26].

The Bohart–Adams adsorption model was applied to experimental data for the description of initial part of the breakthrough curves ($C_t/C_o < 0.5$). The low R^2 values suggested that the model is not as appropriate a predictor for the breakthrough curve as the other models.

4.3.2. Thomas model

Thomas model [27] was used to determine the efficiency of Fe_3O_4–SD adsorbent in a column mode of operation. The model follows the Langmuir kinetics of adsorption–desorption. It assumes negligible axial dispersion of adsorbate within the adsorbent bed inside the column since the adsorption obeys the second-order reversible kinetics [11]. Saturation loading capacity of an adsorbent is important for designing the column. This model was employed to evaluate the saturation loading capacity of the adsorbent in the column. The Thomas model is mathematically expressed as follows:

$$\ln\left(\frac{C_o}{C_t} - 1\right) = \frac{k_{TH}q_e m}{Q} - k_{TH}C_o t \quad (10)$$

where k_{Th} (mL/mg min) is the Thomas rate constant, q_e (mg/g) is the saturation loading capacity of adsorbent, Q is the volumetric flow rate (mL/min), and m is the amount of adsorbent in the column. The values of k_{Th} and q_e can be determined from the linear plot of $\ln[(C_o/C_t) - 1]$ against t. Relative constants and coefficients are presented in Table 3. It was noticed for both the metals that with the increase in feed flow rate, saturation loading capacity decreased but the value of k_{Th} was seen increasing. Similar findings have also been earlier reported [28]. Same trend was observed for metal ion concentration in feed. While q_e and k_{Th} both decreased with increase in adsorbent bed height. The dynamic behavior of the column predicted with Thomas model was in good agreement with experimental data. As it can be seen through the q_e (mg/g) values determined from the experimental values (Table 2) and those calculated from the model (Table 3), the R^2 values showed better suitability of Thomas model for Cu(II) and Ni(II) ions adsorption from aqueous solution using Fe_3O_4–SD. Results indicate that lowest metal concentration in feed, adsorbent bed height, and feed flow rate is favorable for higher adsorption onto Fe_3O_4–SD in fixed-bed column study.

4.3.3. Yoon–Nelson model

This model assumes that the rate of decrease in the probability of adsorption for each adsorbate molecule

Table 3
Dynamic model parameters estimation for Cu(II) and Ni(II) adsorption onto Fe_3O_4–SD

	k_{AB} (L/mg min)		C_S (mg/L)		R^2	
	Cu(II)	Ni(II)	Cu(II)	Ni(II)	Cu(II)	Ni(II)
Bohart–Adams						
Z (cm)						
2	0.0016	0.0017	17,283	12,931.75	0.704	0.671
4	0.0007	0.0009	11,878	11,006.25	0.680	0.843
8	0.0007	0.0006	6,561.19	6,187.31	0.728	0.824
Q (mL/min)						
15	0.0007	0.0007	20,081.43	16,022.39	0.653	0.666
20	0.0016	0.0017	17,283	12,931.75	0.704	0.671
25	0.0008	0.0011	18,628.60	14,618.72	0.739	0.736
C_o *(mg/L)*						
10	0.0007	0.0007	20,081.43	16,022.39	0.653	0.666
20	0.0003	0.0004	18,132.33	14,595.49	0.843	0.813
30	0.0003	0.0004	11,095.68	13,714.06	0.543	0.850
	k_{TH} (ml/min mg)		q_e (mg/g)		R^2	
	Cu(II)	Ni(II)	Cu(II)	Ni(II)	Cu(II)	Ni(II)
Thomas model						
Z (cm)						
2	2.6	2.9	30.56	21.43	0.926	0.909
4	1.2	1.6	20.61	17.76	0.927	0.954
8	1.2	1.2	11.35	10.3	0.909	0.916
Q (mL/min)						
15	1.4	1.4	43.45	33.08	0.883	0.884
20	2.6	2.9	30.56	21.43	0.926	0.909
25	1.5	2.1	22.36	23.57	0.952	0.957
C_o *(mg/L)*						
10	1.4	1.4	43.45	33.08	0.883	0.884
20	2.3	2.6	17.54	13.12	0.888	0.783
30	2.4	3.2	4.77	7.78	0.651	0.701
	k_{YN} (min^{-1})		τ (min) (*exp)		R^2	
	Cu(II)	Ni(II)	Cu(II)	Ni(II)	Cu(II)	Ni(II)
Yoon–Nelson						
Z (cm)						
2	0.026	0.029	764.23 (718.09)	535.86(491.92)	0.926	0.909
4	0.012	0.016	1,030.83 (932.77)	888.12(912.93)	0.927	0.954
8	0.012	0.012	1,135 (1,086.21)	1,030(972.89)	0.909	0.916
Q (mL/min)						
15	0.014	0.014	1,086.42(1,036.54)	827.14(758.38)	0.883	0.884
20	0.026	0.029	764.23 (723.52)	535.86(489.01)	0.926	0.909
25	0.015	0.021	559 (512.22)	392.95(373.98)	0.952	0.957
C_o *(mg/L)*						
10	0.014	0.014	1,086.42(1,031.56)	827.14(769.36)	0.883	0.884
20	0.023	0.026	438.7 (473.81)	328.23(352.02)	0.888	0.783
30	0.024	0.032	119.54 (290.97)	194.53(219.65)	0.651	0.701

is proportional to the probability of adsorbate adsorption and adsorbate breakthrough on the adsorbent [29].

$$\ln\left(\frac{C_t}{C_o - C_t}\right) = k_{YN}t - \tau k_{YN} \quad (11)$$

where k_{YN} (min^{-1}) is the rate constant and τ is the time required for 50% adsorbate breakthrough.

The value of τ obtained experimentally is given in Table 3. As shown in Table 3, values of k_{YN} were found to increase with increasing feed flow rate and metal ion concentration in feed solution while τ showed the reverse trend for Cu(II) and Ni(II) adsorption using Fe_3O_4–SD. For the increasing adsorbent bed height, k_{YN} decreased while τ increased. Same pattern was reported in the previous research [30]. The time required for 50% adsorbate breakthrough obtained from the Yoon and Nelson model agreed well with the experimental data at all conditions examined. Through values of R^2, it can be concluded that both the Thomas and Yoon–Nelson models can predict adsorption performance satisfactorily.

4.4. Desorption experiments

Desorption flow experiments were conducted on the saturated adsorbent contained in the column. Regeneration of adsorbent for loaded metal recovery was done using acid elution, and 0.1 N HCl was used for this purpose. For the first adsorption cycle, the solution containing 10 mg/L of Cu(II) and Ni(II) ions was made to flow through the 2-cm adsorbent bed at 15 mL/min. Desorption with 0.1 N HCl was for 500 min. In the next adsorption cycle under the same conditions (as for the first cycle), it was noticed that the adsorption capacity decreased from 31.89 to 28.2 mg/g for Cu(II) and 23.59 to 18 mg/g for Ni(II) ions. From desorption results, it could be depicted that ion—exchange mechanism is the satisfactory mechanism for the purpose of regeneration of adsorbent [31].

5. Conclusion

The study highlights the combined removal of Cu (II) and Ni(II) ions using Fe_3O_4–SD nano-particles in a fixed-bed column. Maximum adsorption capacity (31.89 mg/g for Cu(II) and 23.59 mg/g for Ni(II)) was noticed for solution containing 10 mg/L of both the metals at a pH 5 when passed through a column with 2 cm of adsorbent bed height. The breakthrough time increased with increase in bed height of adsorbent. The H_{UNB} and MTZ height were found to be increasing with increase in feed flow rate, adsorbent bed height, and metal ion concentration in feed solution. The main mechanism of adsorption was complexation and ion exchange due to the presence of Fe–O and –OH bonds on the adsorbent surface. Yoon–Nelson and Thomas models were found to give good fit to adsorption data. Thus, Fe_3O_4–SD has a potential of removing cationic species Cu(II) and Ni(II) ions from the aqueous stream in a dynamic mode of operation.

Acknowledgments

Authors are thankful to Indian Institute of Technology (Banaras Hindu University), India, for extending all necessary facilities and supports to undertake the work.

References

[1] S.E. Bailey, T.J. Olin, R.M. Bricka, D. Adrian, A review of potentially low-cost sorbents for heavy metals, Water Res. 33 (1999) 2469–2479.
[2] U. Kumar, M. Bandyopadhyay, Sorption of cadmium from aqueous solution using pretreated rice husk, Bioresour. Technol. 97 (2006) 104–109.
[3] H.J.M. Bowen. The Environmental Chemistry of the Elements, Academic Press, London, 1979.
[4] M.C. Linder, M.H. Azam, Copper biochemistry and molecular biology, Am. J. Clin. Nutr. 63 (1996) 797S–811S.
[5] N.C. Brady, R.R. Weil, The Nature and Properties of Soil, Prentice Hall, Technology & Engineering, Upper Saddle River, NJ, 1996.
[6] J. Gerendás, J.C. Polacco, S.K. Freyermuth, B. Sattelmacher, Significance of nickel for plant growth and metabolism, J. Plant Nutr. Soil Sci. 162(3) (1999) 241–256.
[7] D. Bulgariu, L. Bulgariu, Equilibrium and kinetics studies of heavy metal ions biosorption on green algae waste biomass, Bioresour. Technol. 103 (2011) 489–493.
[8] M. Kapur, M.K. Mondal, Adsorption kinetics and isotherms for Cu(II) and Ni(II) ions removal from electroplating industrial wastewater, IJAER 9(1) (2014) 47–52.
[9] Y. Zhang, C. Banks, A comparison of the properties of polyurethane immobilized Sphagnum moss, seaweed, sunflower waste and maize for the biosorption of Cu, Pb, Zn and Ni in continuous flow packed columns, Water Res. 40 (2006) 788–798.
[10] M.A. Acheampong, K. Pakshirajan, A.P. Annachhatre, P.N.L. Lens, Removal of Cu(II) by biosorption onto coconut shell in fixed-bed column systems, J. Ind. Eng. Chem. 19 (2013) 841–848.
[11] C.M. Futalan, C.C. Kan, M.L. Dalida, C. Pascua, M.W. Wan, Fixed-bed column studies on the removal of copper using chitosan immobilized on bentonite, Carbohydr. Polym. 83 (2011) 697–704.

[12] F. Ji, C. Li, J. Xu, P. Liu, Dynamic adsorption of Cu(II) from aqueous solution by zeolite/cellulose acetate blend fiber in fixed-bed, Colloids Surf., A 434 (2013) 88–94.
[13] N.K.E.M. Yahaya, I. Abustan, M.F.P.M. Latiff, O.S. Bello, M.A. Ahmad, Fixed-bed column study for Cu (II) removal from aqueous solutions using rice husk based activated Carbon, IJET-IJENS 11 (2011) 248–252.
[14] K.A. Anoop Krishnan, K.G. Sreejalekshmi, R.S. Baiju, Nickel(II) adsorption onto biomass based activated carbon obtained from sugarcane bagasse pith, Bioresour. Technol. 102 (2011) 10239–10247.
[15] E. Malkoc, Y. Nuhoglu, Removal of Ni(II) ions from aqueous solutions using waste of tea factory: Adsorption on a fixed-bed column, J. Hazard. Mater. 135 (2006) 328–336.
[16] S. Chamarthy, C.W. Seo, W.E. Marshall, Adsorption of selected toxic metals by modified peanut shells, J. Chem. Technol. Biotechnol. 76 (2001) 593–597.
[17] M.K. Mondal, Removal of Pb(II) ions from aqueous solution using activated tea waste: Adsorption on a fixed-bed column, J. Environ. Manage. 90 (2009) 3266–3271.
[18] M. Kapur, M.K. Mondal, Mass transfer and related phenomena for Cr(VI) adsorption from aqueous solutions onto *Mangifera indica* sawdust, Chem. Eng. J. 218 (2013) 138–146.
[19] V.K. Gupta, A. Nayak, Cadmium removal and recovery from aqueous solutions by novel adsorbents prepared from orange peel and Fe_2O_3 nanoparticles, Chem. Eng. J. 180 (2012) 81–90.
[20] Standard Methods for Examination of Water and Wastewater, fourteenth ed., APHA, AWWA WPCF, Washington, DC, 1975.
[21] Z. Aksu, F. Gönen, Biosorption of phenol by immobilized activated sludge in a continuous packed bed: prediction of breakthrough curves, Process Biochem. 39 (2004) 599–613.
[22] V.K. Gupta, S. Agarwal, T.A. Saleh, Chromium removal by combining the magnetic properties of iron oxide with adsorption properties of carbon nanotubes, Water Res. 45 (2011) 2207–2212.
[23] N. Sankararamakrishnan, P. Kumar, V.S. Singh Chauhan, Modeling fixed bed column for cadmium removal from electroplating wastewater, Sep. Purif. Technol. 63 (2008) 213–219.
[24] M. Jain, V.K. Garg, K. Kadirvelu, Cadmium(II) sorption and desorption in a fixed bed column using sunflower waste carbon calcium-alginate beads, Bioresour. Technol. 129 (2013) 242–248.
[25] J. Goel, K. Kadirvelu, C. Rajagopal, V.K. Kumar Garg, Removal of lead(II) by adsorption using treated granular activated carbon: Batch and column studies, J. Hazard. Mater. 125 (2005) 211–220.
[26] E.I. Unuabonah, M.I. El-Khaiary, B.I. Olu-Owolabi, K.O. Adebowale, Predicting the dynamics and performance of a polymer–clay based composite in a fixed bed system for the removal of lead(II) ion, Chem. Eng. Res. Des. 90 (2012) 1105–1115.
[27] H.C. Thomas, Heterogeneous ion exchange in a flowing system, J. Am. Chem. Soc. 66 (1944) 1664–1666.
[28] S. Sadaf, H.N. Bhatti, Batch and fixed bed column studies for the removal of Indosol Yellow BG dye by peanut husk, J. Taiwan Inst. Chem. Eng. 45 (2014) 541–553.
[29] Y.H. Yoon, J.H. Nelson, Application of gas adsorption kinetics I. A theoretical model for respirator cartridge service life, Am. Ind. Hyg. Assoc. J. 45 (1984) 509–516.
[30] M. Bhaumik, K. Setshedi, A. Maity, M.S. Onyango, Chromium(VI) removal from water using fixed bed column of polypyrrole/Fe_3O_4 nanocomposite, Sep. Purif. Technol. 110 (2013) 11–19.
[31] S.S. Baral, N. Das, T.S. Ramulu, S.K. Sahoo, S.N. Das, G. Chaudhury, Removal of Cr(VI) by thermally activated weed *Salvinia cucullata* in a fixed-bed column, J. Hazard. Mater. 161 (2009) 1427–1435.